Refinement of the grain size of the LM25 alloy (A356) by 96Al–2Nb–2B master alloy

L. Bolzoni*, N. Hari Babu

Brunel University London, Institute of Materials and Manufacturing, Kingston Lane, Uxbridge UB8 3PH, Middlesex, UK

A B S T R A C T

Nb-based intermetallics contained in the master alloy act as potent heterogeneous nucleation substrate for the nucleation of primary Al dendrites. The addition of the 96Al–2Nb–2B master alloy to the LM25 alloy permits to significantly refine its microstructural features and the refinement is achieved in a great range of cooling rates. The formation of columnar grains at slow cooling rates is prevented.

© 2015 The Authors. Published by Elsevier B.V. This is an open access article under the CC BY license (http://creativecommons.org/licenses/by/4.0/).

1. Introduction

The refining treatment on hypo-eutectic Al–Si alloy is practically convenient and this is normally carried out by the addition of commercial master alloys developed on the Al–Ti–X (where X = B or C) ternary system (Mayes et al., 1993). The influence of the ratio between Ti and B was considered by Sritharan and Li (1997), the employment of Ti and B salts studied by Henghua et al. (2006) and the combined effect of grain refinement and semi-solid processing analysed by Nafisi and Ghomashchi (2006). Although of the over 50 years research and industrial practise (McCartney, 1989) over which many different theories explaining the grain refining mechanism have been proposed (Easton and St. John, 1999), there are still some controversies. The most plausible nucleation theory suggests that TiB_2 particles need to be coated with thin layer of Al_3Ti to be effective nucleant particles (Schumacher and Mc Kay, 2003). The Al–Ti–X commercial master alloys are highly effective in refining pure aluminium and wrought aluminium alloys (whose silicon content is generally lower than 3 wt.%) due to both the nucleation potency of the Ti-compounds and the high growth restriction factor of titanium on aluminium. The employment of commercial Al–Ti–X master alloys for the refinement of Al–Si cast alloys, although done, is not very effective because of the poisoning effect that silicon has on titanium as described by Kori et al. (2005). Quested at al. studied the poisoning effect from a thermodynamic point of view

(Quested et al., 2006). In particular, on increasing the silicon addition to aluminium, the grain size passes through a minimum that occur at 0.5–7 wt.% Si depending on conditions, but is typically ∼3–4 wt.% Si (Johnsson and Bäckerud, 1994). The mechanism governing the poisoning (i.e. formation of titanium silicides) is not completely understood but its effects are very clear. The melt is depleted of titanium and the potency of TiB_2 particles as heterogeneous nucleation sites is greatly diminished; consequently, grain refinement is not achieved reliably. The scientific community has proposed some variants and alternatives, such as the employment of sub-stoichiometric compositions, replacement of B with C and employment of Al–B master alloys (Li et al., 1997), all of them based on the Al–Ti–X system. We focused on the replacement of titanium, the element that is actually causing problem, and came up with a chemical composition that can efficiently refine the microstructure of Al–Si alloys. Starting from the study of the addition of pure Nb and/or B on binary Al–Si alloys (Nowak et al., 2015) as well as commercial alloys (Bolzoni et al., 2015b), it was shown that their effect is much greater than addition of the individual elements (i.e. Nb or B alone) (Bolzoni et al., 2015c). In this manuscript the refining performances of one of these master alloys (i.e. the 96Al–2Nb–2B master alloy) on the microstructural features and mechanical properties of the hypo-eutectic LM25 (A356) alloy are addressed, presented and discussed in details.

2. Experimental procedure

The 96Al–2Nb–2B master alloy was produced by mixing pure aluminium with Nb powder and a 95Al–5B master alloy. The

---

* Corresponding author. Tel.: +44 1895 267202; fax: +44 1895 269758.
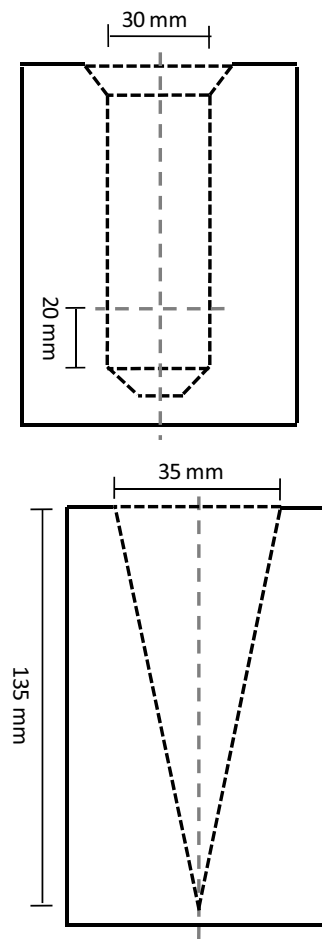*E-mail address:* leandro.bolzoni@brunel.ac.uk (L. Bolzoni).

Fig. 1. Sketch of the moulds used during the study: (a) 30 mm cylindrical steel mould and (b) wedge-shape copper mould.

Fig. 2. Comparison of the cooling curves of the LM25 alloy without and with Nb–B inoculation.

Table 1
Data obtained from the analysis of the cooling curves shown in Fig. 1.

Temperature	Reference	96Al–2Nb–2B addition
$T_{minimum}$ [°C]	617.9	617.8
T_{growth} [°C]	619.6	618.4
Undercooling, ΔT [°C]	1.7	0.6

details of the production and characterisation of this master alloy composed of Nb-based compounds are available in a previous publication (Bolzoni et al., 2015a). The effect of Nb–B inoculation on the solidification mechanism was studied by quantifying the undercooling obtaining cooling curves in slow cooled materials; data were collected using type-K thermocouples connected to a data logger. It has been reported that thermal analysis is a useful tool to understand the effect of the addition of grain refiners. Murty et al. (2002) said that thermal analysis has been used to assess the performance of grain refiners in the case of a number of foundry alloys and Spittle (2008) specified that the features of the shape of a thermal analysis curve accompanying supercooling and recalescence, relate to grain refining potential. For the grain refinement experiments the LM 25 alloy (A356), whose silicon content is ~7 wt.%, Mg = 0.3 wt.%, Fe = 0.5 wt.% and Ti = 0.11 wt.%, was melt at 790 °C. Afterwards, either the alloy was cooled at 740 ± 3 °C and cast (reference) or the 96Al–2Nb–2B master alloy (level of addition of 0.1 wt.% equivalent of Nb) was added 30 min before casting (i.e. contact time) prior to follow the same casting procedure. Somewhat lower Nb content with respect to the targeted value is, anyway, expected because some Nb got oxidised during the fabrication of the 96Al–2Nb–2B master alloy. The moulds used during the study are sketch in Fig. 1.

The cooling rate range considered by means of the setup used varies in between 2 °C/s (cylindrical steel mould) up to 1000 °C/s (i.e. tip of the wedge-shape copper mould). It is worth mentioning that the microstructural analysis was performed on the cross-section of bot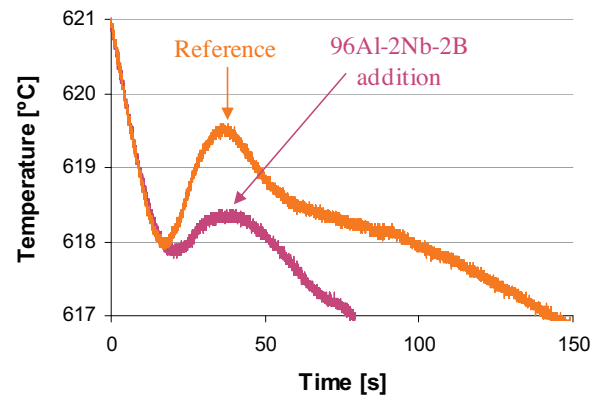h the cylindrical samples (at 20 mm from the bottom) and of the wedge-shaped specimens (whole section). Visual inspection (macro analysis) of the refinement effect was done on grinded and etched (Tucker's reagent) samples whilst microstructural analysis was carried out on either polished samples (obtained by means of the conventional metallographic route) or anodised (Barker's solution) specimens. The measurements of the grain size were done in a Carl Zeiss Axioskop-2-MAT microscope using the linear intercept method.

3. Results and discussion

The comparison of the cooling curves of the LM25 alloy without and with the addition of the 96Al–2Nb–2B master alloy and the results of their analysis are reported in Fig. 2 and Table 1, respectively.

From Fig. 2, the reference alloy cools down to roughly 618 °C and due to the thermodynamic barrier to nucleation it undercools before the formation of any agglomeration of (solid solution of) aluminium able to survive in the supercooled molten metal. Because of the slow cooling employed during the thermal analysis, the primary aluminium grains start to growth the temperature raises reaching a peak, known as recalescence. As indicated by Knuutinen et al. (2001), it should be noted that ΔT is sometimes denoted as undercooling, where $\Delta T = T_{minimum} - T_{growth}$. From the comparison of the cooling curve of the material without and with 96Al–2Nb–2B master alloy addition, it can be seen that the shape of the curves is not changed and the minimum temperatures are comparable but the recalescence temperature, and consequently, the undercooling after the addition of the 96Al–2Nb–2B master alloy is lower. The reduction of the undercooling generated along the solidification of the material suggests that heterogeneous nucleation is the governing mechanism because an ideal substrates for nucleation will reduce the undercooling at zero (Apelian et al., 1984). Nb–B inoculation was chosen because Nb-based intermetallic compounds have good lattice match with the cubic crystal structure of Al (Nowak et al., 2015). In the discussion of the nucleation phenomena, Fredriksson and Åkerlind (2012) asserted that the undercooling is proportional to the square of the (lattice) mismatch and some conditions must be fulfilled among which: the compound must not dissolve in the melt and the interface between low-index
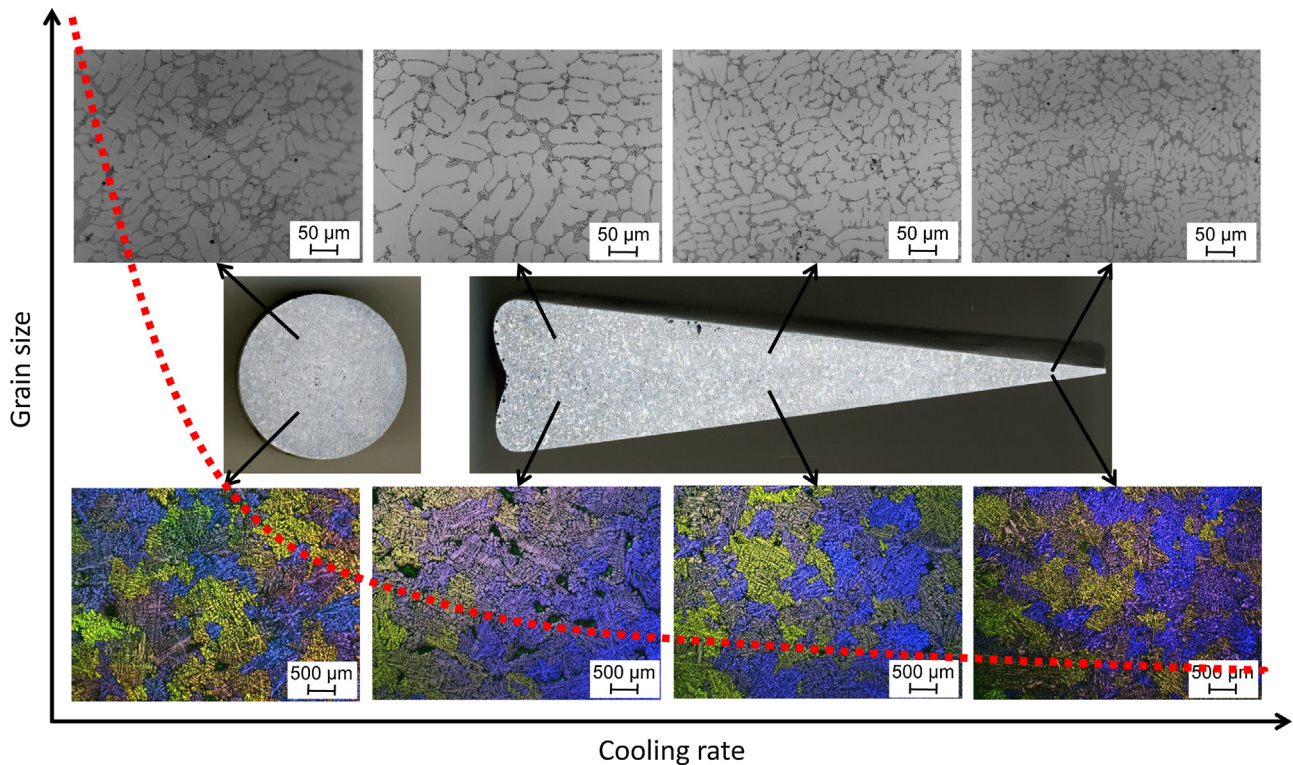
Fig. 3. Representative macro- and microstructural images of the LM25 alloy (reference); top: details of the eutectic phase, middle: macro-etched cross-sections and bottom: anodised micrographs.

planes of the substrate and the nucleated solid must be coherent or nearly coherent. The low lattice mismatch and the reduction of the undercooling suggest that a coherent or semi coherent interface is present between the Nb-based intermetallics and the nucleation aluminium grains.

Fig. 3 shows representative macro- and microstructural images of the LM 25 alloy without the addition of any grain refiner (reference).

From Fig. 3, the variation of the grain size (i.e. size of the primary α-Al dendrites, bottom micrographs) with the cooling rate can be represented with an asymptotic curve. This behaviour is the expected one because the lower the cooling rate the greater the time for the growth of the grain that nucleated, most probably, from the walls of the die. The very fast cooling rate available of the tip of the wedge-shaped samples (i.e. in the order of 100–1000 °C/s) leads to the formation of fine equiaxed Al grains of approximately 400 μm. In the middle of the wedge-shaped samples, at intermediate cooling rate, the grain size is in the order of 750 μm reaching around 1000 μm in the wider part. A further increment of the grain size (~1190 μm) is obtained in the microstructure of the cylindrical specimens whose cooling rate is somewhat lower. Concerning the eutectic Al–Si phase (top micrographs), it can be noticed that its distribution becomes less even with the lowering if the cooling rate. This is because the eutectic phase nucleates from the solute enriched molten metal which remains after the nucleation of the primary α-Al dendrites and, consequently, it is found in between the arms of the dendrites. The bigger the dendritic grains become, the more confined the eutectic phase is. It is worth mentioning that the morphology of the eutectic phase is modified from planar (i.e. needle-shape morphology) to fibrous because the starring materials already included some addition of strontium. Due to the relatively low silicon content of the LM25 alloy, no primary Si particles are present in the microstructures. Others microstructural features present in this alloy are the needle-shaped and

script-like Fe-based intermetallics whose size/length increases with the decreasing of the cooling rate.

Representative micrographs concerning the LM25 alloy with the addition of the Nb-based compounds by means of the 96Al–2Nb–2B master alloy are reported in Fig. 4.

From Fig. 4, the shape of the trend of the variation of the grain size does not change after the addition of the 96Al–2Nb–2B master alloy because it is still characterised by an asymptotic behaviour (bottom micrographs). The variation of the grain size is significantly lower in comparison to the reference material (Fig. 3). The size of the primary α-Al equiaxed grain at very fast cooling rate (tip of the wedge-shaped sample) is very fine (less than 80 μm) due to the combined effect of high cooling rate and heterogeneous nucleation by the 96Al–2Nb–2B master alloy. Moving towards slower cooling rates (from middle to wide part of the wedge-shaped sample) the size of the α-dendrites slightly increases to around 250–330 μm. These values of the grain size are much smaller with respect to those found in the reference material (in the order of mm) and clearly indicate the effect of the addition of the 96Al–2Nb–2B master alloy to the LM25 alloy. A further decrement of the cooling rate leads to the further coarsening of the microstructure (approximately 350 μm for the cylindrical mould specimen) but the final grain size is still much finer than the reference. With respect to the Al–Si intermetallic phase (top micrographs), the addition of the Nb-based compounds to promote the heterogeneous nucleation of the primary α-Al dendrites leads to a better and more even distribution. This is thought to be a consequence of the smaller space available in between the dendritic arms of the growing crystals as well as to the lower partitioning of the alloying elements (especially silicon) in the melt pools. The size of the eutectic phase is generally somewhat finer most probably due to the greater number of α-Al grains from which the Al–Si eutectic phase can nucleate (i.e. similar lattice parameters). The less heterogeneous distribution of the alloying elements during the solidification process obtained by the addition
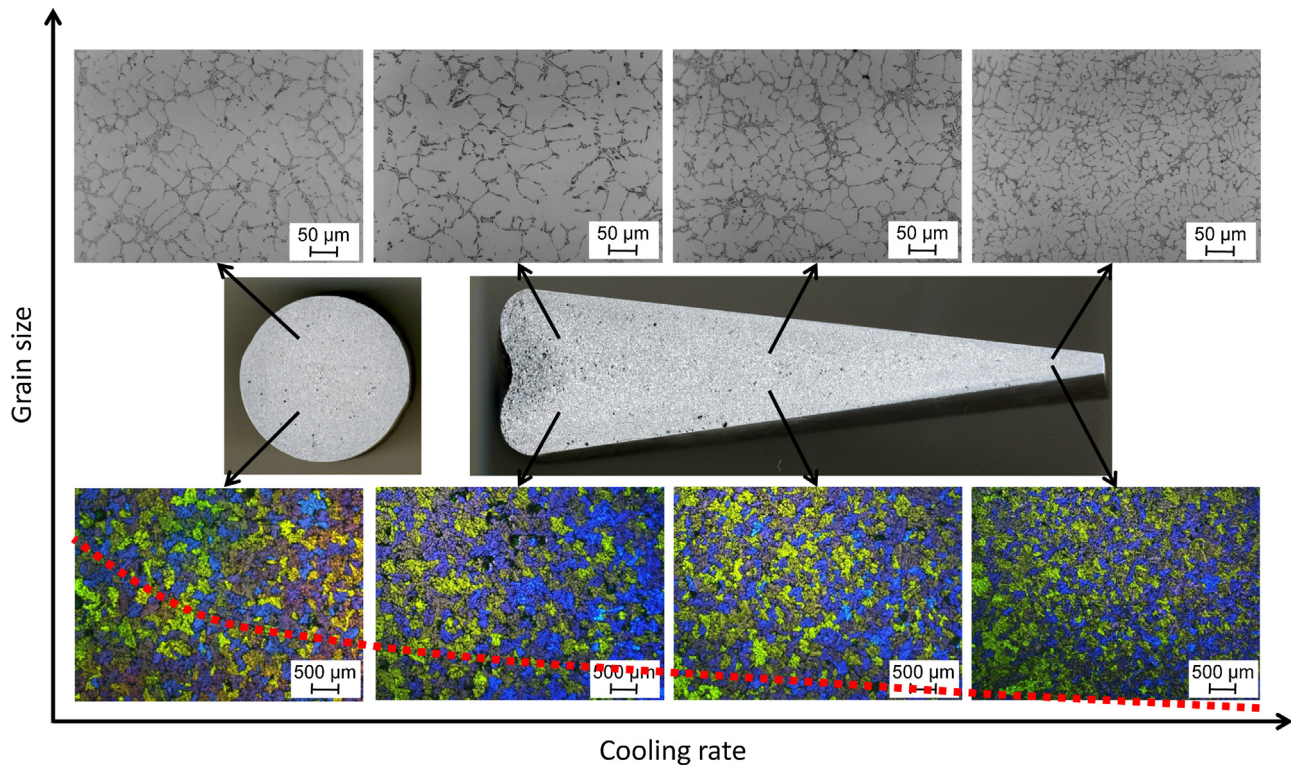
Fig. 4. Representative macro- and microstructural images of the LM25 alloy after the addition of the 96Al–2Nb–2B master alloy; top: details of the eutectic phase, middle: macro-etched cross-sections and bottom: anodised micrographs.

of the 96Al–2Nb–2B master alloy results also in the formation of finer and less interconnected Fe-based intermetallics dispersed in the microstructure. The refinement of the microstructural features (i.e. grain size, intermetallic phase and Fe-based intermetallics) by means of the 96Al–2Nb–2B master alloy is mainly due to the presence of Nb-based compounds, specifically niobium borides and niobium aluminides. Niobium borides are intermetallic particles characterised by a hexagonal structure whose lattice parameters are quite similar to that of aluminium. As in the case of Al–Ti–B master alloys for wrought aluminium alloys, it is believed that a layer of (niobium) aluminide is formed on top of the borides particles where this Al_3Nb has a tetragonal structure with accommodated lattice parameters which are much more similar to those of aluminium and, consequently, significantly enhance the heterogeneous nucleation of the primary α-Al dendrites. As it can be inferred, TiB-based and Nb-based compounds are characterised by the same atomic structure and similar lattice parameters but they differ in a critical aspect: Nb-compounds can efficiently refine the microstructural features of Al–Si cast alloys. The reason of this difference is related to the stability of the compounds in presence of silicon. Titanium reacts very easily with silicon to form silicides (poisoning) whilst niobium does it far less and this is due to the fact that there are less niobium silicides that can form (3 against 5 as per binary phase diagrams, ASM International, 1992) and they are stable at much higher temperature (Zhao et al., 2004).

The variation of the grain size with the cooling rate is displayed in Fig. 5 along with the relative prediction calculated using the approximation that the average grain size y (of the LM25 alloy) depends on the cooling rate x according to (Flemings, 1974):

$$y = \beta \times (x)^{-m} \tag{1}$$

where β and m are factors that varies with the nature of the alloy and of the solidification conditions.

The plotting of the data on semi-log diagram permits to clearly understand the variation of the grain size of the LM25 alloy with the
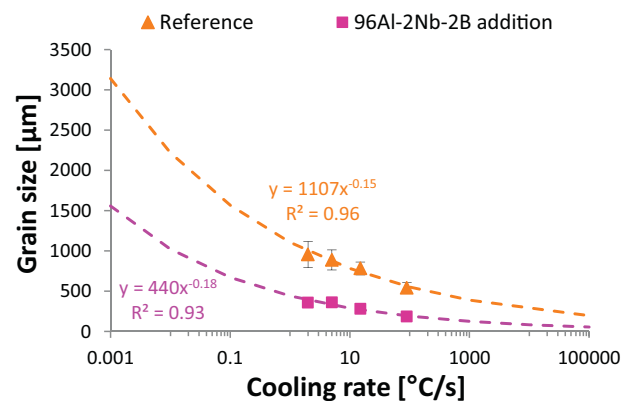

Fig. 5. Grain size and efficacy vs. cooling rate f for the LM25 alloy without and with the addition of the 96Al–2Nb–2B master alloy.

cooling rate (decreases exponentially) as well as see that the difference in between the size of the primary α-Al dendrites without with Nb–B inoculation becomes greater towards equilibrium cooling conditions. This aspect indicates that the presence of the Nb-based heterogeneous nucleation substrates introduced by means of the addition of the 96Al–2Nb–2B master alloy becomes more substantial when the alloy is solidified using slow cooling rates. In practical terms, Nb–B inoculation will, most probably, be more justified for sand casting products (cooling rate in the order of Celsius degrees) than for high-pressure die casting components (cooling rate in the order of hundreds/thousand Celsius degrees).

4. Conclusions

From the addition of the 96Al–2Nb–2B master alloy to the LM25 alloy it is concluded that:

- Nb-based intermetallics are good substrates for the heterogeneous nucleation of aluminium grains.
- The microstructural features (grain size, eutectic phase and secondary phases) are significantly refined.
- The refinement is achieved over a great cooling rate range.
- The formation of columnar grains at slow cooling rates is prevented.
- A less heterogeneous distribution of the eutectic phase which lays in between the dendritic arms is obtained.

Acknowledgements

References

Apelian, D., Sigworth, G.K., Whaler, K.R., 1984. Assessment of grain refinement and modification of Al–Si foundry alloys by thermal analysis. AFS Trans. 92, 297–307.

ASM International, 1992. ASM Handbook Volume 03: Alloy Phase Diagrams. ASM International, Ohio.

Bolzoni, L., Nowak, M., Hari Babu, N., 2015a. Assessment of the influence of Al–2Nb–2B master alloy on the grain refinement and properties of LM6 (A413) alloy. Mater. Sci. Eng., A 628, 230–237.

Bolzoni, L., Nowak, M., Hari Babu, N., 2015b. Grain refinement of Al–Si alloys by Nb–B inoculation. Part II: Application to commercial alloys. Mater. Des. 66, 376–383.

Bolzoni, L., Nowak, M., Hari Babu, N., 2015c. Grain refining potency of Nb–B inoculation on Al–12Si–0.6Fe–0.5Mn alloy. J. Alloys Compd. 623, 79–82.

Easton, M., St. John, D.H., 1999. Grain refinement of aluminum alloys: Part I. The nucleant and solute paradigms—a review of the literature. Metall. Mater. Trans. A: Phys. Metall. Mater. Sci. 30, 1613–1623.

Flemings, M.C., 1974. Solidification Processing. McGraw-Hill, NY, USA.

Fredriksson, H., Åkerlind, U., 2012. Solidification and Crystallization Processing in Metals and Alloys. Wiley, West Sussex, UK.

Henghua, Z., Xuan, T., Guangjie, S., Luoping, X., 2006. Refining mechanism of salts containing Ti and B elements in purity aluminum. J. Mater. Process. Technol. 180, 60–65.

Johnsson, M., Bäckerud, L., 1994. The influence of composition on equiaxed crystal growth mechanisms and grain size in Al alloys. Zeitschrift für Metallkunde 85, 781–785.

Knuutinen, A., Nogita, K., McDonald, S.D., Dahle, A.K., 2001. Modification of Al–Si alloys with Ba, Ca, Y and Yb. J. Light Met. 1, 229–240.

Kori, S.A., Auradi, V., Murty, B.S., Chakraborty, M., 2005. Poisoning and fading mechanism of grain refinement in Al–7Si alloy. Mater. Forum 29, 387–393.

Li, H., Sritharan, T., Lam, Y.M., Leng, N.Y., 1997. Effects of processing parameters on the performance of Al grain refinement master alloys Al–Ti and Al–B in small ingots. J. Mater. Process. Technol. 66, 253–257.

Mayes, C.D., McCartney, D.G., Tatlock, G.J., 1993. Influence of microstructure on grain refining performance of Al–Ti–B master alloys. Mater. Sci. Technol. 9, 97–103.

McCartney, D.G., 1989. Grain refining of aluminium and its alloys using inoculants. Int. Mater. Rev. 34, 247–260.

Murty, B.S., Kori, S.A., Chakraborty, M., 2002. Grain refinement of aluminium and its alloys by heterogeneous nucleation and alloying. Int. Mater. Rev. 47, 3–29.

Nafisi, S., Ghomashchi, R., 2006. Grain refining of conventional and semi-solid A356 Al–Si alloy. J. Mater. Process. Technol. 174, 371–383.

Nowak, M., Bolzoni, L., Hari Babu, N., 2015. Grain refinement of Al–Si alloys by Nb–B inoculation. Part I: Concept development and effect on binary alloys. Mater. Des. 66, 366–375.

Quested, T.E., Dinsdale, A.T., Greer, A.L., 2006. Thermodynamcs evidence for a poisoning mechanism in the Al–Si–Ti system. Mater. Sci. Technol. 22, 1126–1134.

Schumacher, P., Mc Kay, B.J., 2003. TEM investigation of heterogeneous nucleation mechanisms in Al–Si alloys. J. Non-Cryst. Solids 317, 123–128.

Spittle, J.A., 2008. Grain refinement in shape casting of aluminium alloys—Part I. FTJ 10, 308–314.

Sritharan, T., Li, H., 1997. Influence of titanium to boron ratio on the ability to grain refine aluminium–silicon alloys. J. Mater. Process. Technol. 63, 585–589.

Zhao, J.C., Jackson, M.R., Peluso, L.A., 2004. Mapping of the Nb–Ti–Si phase diagram using diffusion multiples. Mater. Sci. Eng., A 372, 21–27.